ELSEVIER

Since January 2020 Elsevier has created a COVID-19 resource centre with free information in English and Mandarin on the novel coronavirus COVID-19. The COVID-19 resource centre is hosted on Elsevier Connect, the company's public news and information website.

More tools for our toolkit: The application of HEL-299 cells and dsRNA-nanoparticles to study human coronaviruses in vitro

Shawna L Semple [a], Tamiru N Alkie [a], Kristof Jenik [a], Bryce M Warner [b], Nikesh Tailor [b], Darwyn Kobasa [b], Stephanie J DeWitte-Orr [a,*]

[a] *Department of Biology, Wilfrid Laurier University, Waterloo, ON, Canada*
[b] *Public Health Agency of Canada, Winnipeg, Manitoba, Canada*

ARTICLE INFO

ABSTRACT

Human coronaviruses (HCoVs) are important human pathogens, as exemplified by the current SARS-CoV-2 pandemic. While the ability of type I interferons (IFNs) to limit coronavirus replication has been established, the ability of double-stranded (ds)RNA, a potent IFN inducer, to inhibit coronavirus replication when conjugated to a nanoparticle is largely unexplored. Additionally, the number of IFN competent cell lines that can be used to study coronaviruses *in vitro* are limited. In the present study, we show that poly inosinic: poly cytidylic acid (pIC), when conjugated to a phytoglycogen nanoparticle (pIC+NDX) is able to protect IFN-competent human lung fibroblasts (HEL-299 cells) from infection with different HCoV species. HEL-299 was found to be permissive to HCoV-229E, -OC43 and MERS-CoV-GFP but not to HCoV-NL63 or SARS-CoV-2. Further investigation revealed that HEL-299 does not contain the required ACE2 receptor to enable propagation of both HCoV-NL63 and SARS-CoV-2. Following 24h exposure, pIC+NDX was observed to stimulate a significant, prolonged increase in antiviral gene expression (IFNβ, CXCL10 and ISG15) when compared to both NDX alone and pIC alone. This antiviral response translated into complete protection against virus production, for 4 days or 7 days post treatment with HCoV-229E or -OC43 when either pre-treated for 6h or 24h respectively. Moreover, the pIC+NDX combination also provided complete protection for 2d post infection when HEL-299 cells were infected with MERS-CoV-GFP following a 24h pretreatment with pIC+NDX. The significance of this study is two-fold. Firstly, it was revealed that HEL-299 cells can effectively be used as an IFN-competent model system for *in vitro* analysis of MERS-CoV. Secondly, pIC+NDX acts as a powerful inducer of type I IFNs in HEL-299, to levels that provide complete protection against coronavirus replication. This suggests an exciting and novel area of investigation for antiviral therapies that utilize innate immune stimulants. The results of this study will help to expand the range of available tools scientists have to investigate, and thus further understand, human coronaviruses.

1. Introduction

Human coronaviruses (HCoVs) were an unknown entity until 1966 when Tyrell and Bynoe isolated an ether-sensitive virus from the respiratory tract of an adult presenting cold-like symptoms (Tyrrell and Bynoe, 1966). At that time, several other researchers had also reported the detection of viruses that induced mild upper respiratory tract infections in humans (Hamre and Procknow, 1966; McIntosh et al., 1967). These pathogens did not share the defining features of other cold-causing, enveloped viruses and also differed significantly in morphology when viewed by electron microscopy (Almeida and Tyrrell, 1967). This eventually led to the recognition of a new family of viruses called *Coronaviridae*, so named due to the "crown"- or "corona"-like appearance of their surface projections, now known as spike proteins (Tyrrell et al., 1975). Since then, there have been seven HCoV species identified. The four common species are HCoV-229E, -OC43, -NL63, and -HKU1. These typically cause mild to moderate upper-respiratory tract ailments resulting in approximately 15-30% of common colds (reviewed by Van der Hoek, 2007). In contrast, a highly pathogenic illness known as severe acute respiratory syndrome (SARS) is caused by the three remaining HCoV species: SARS-1, MERS-CoV and SARS-CoV-2 (reviewed by da Costa et al., 2020). SARS is defined as a highly transmissible, febrile lower respiratory tract infection often leading to pneumonia and/or acute respiratory distress (reviewed by Christian

---

et al., 2004). Following their discovery, each of the three SARS-associated viruses have been responsible for significant casualties and morbidities. Indeed, the current COVID-19 pandemic caused by SARS-CoV-2 has resulted in serious global economic and public health consequences while also highlighting the need for a deeper understanding of fundamental HCoV interactions with the immune system (reviewed in Hu et al., 2020). As such, more cellular and molecular tools are needed to better study this group of viruses.

For any virus to successfully replicate, permissive host cells must contain receptors that facilitate viral attachment and subsequent entry. With respect to HCoVs, binding of their spike protein enables access into target cells where the virus can then exploit host cellular machinery to ensure its replication (reviewed by Chen et al., 2020). However, not all of the HCoV species require the same receptor (reviewed by Guruprasad, 2021). HCoV-NL63, SARS-1 and SARS-CoV-2 bind to angiotensin-converting enzyme 2 (ACE2), HCoV-HKU1 and -OC43 utilize 9-O-acetylated sialic acid (9-O-Ac-Sia), HCoV-229E uses aminopeptidase N (CD13), and MERS-CoV binds to dipeptidyl peptidase 4 (CD26) to enable entry into human cells (Yeager et al., 1992; Hulswit et al., 2019; reviewed by Guruprasad, 2021). Due to this varied receptor tropism, *in vitro* studies involving HCoVs often use a variety of different cell lines. This can often make it difficult to understand HCoVs as well as their interactions with cellular immune defenses.

Double-stranded (ds)RNA is a by-product of viral replication and a potent inducer of type I interferons (IFNs) (Weber et al., 2006; Son et al., 2015; Li et al., 2021). Because long dsRNA is not found in normal, healthy cells, this molecule is able to act as a pathogen associated molecular pattern (PAMP) and can alert the host immune system to the presence of viral pathogens (reviewed by Kawai and Akira, 2006). To do this, long dsRNA binds to host pattern recognition receptors (PRRs) such as toll-like receptor (TLR)-3 within the endosome as well as retinoic acid-inducible gene -I (RIG-I) and melanoma differentiation-associated protein 5 (MDA5) within the cytoplasm (reviewed by Brennan and Bowie, 2010). Upon receptor binding, signaling pathways are activated resulting in the production of type I intererons (IFNs). These IFNs signal through their cognate receptor (IFNAR) and the Jak/STAT pathway to activate hundreds of interferon stimulated genes (ISGs) including CXCL10 and ISG15 (reviewed by Yang and Li, 2020). An accumulation of ISGs within a cell establishes an antiviral state, making the cell refractory to viral infection (reviewed in Borden et al., 2007; Perng and Lenschow, 2018). To date, it has been shown that coronaviruses produce dsRNA during replication (Hagemeijer et al., 2012) which activates TLR-3, RIG-I, and MDA5 signaling pathways (Totura et al., 2015; Sampaio et al., 2021; Yamada et al., 2021). Type I IFNs can be effective at limiting HCoV replication and treatment prior to peak replication may provide effective protection against SARS-CoV-2 (reviewed by Sodeifian et al. 2022). However, the coronavirus/IFN interaction is complicated. HCoVs, such as SARS-CoV-2, are poor inducers of IFNs *in vivo*, which suggests effective immune evasion strategies (Chu et al., 2020). Indeed, SARS-CoV-2 encodes for at least 10 proteins that interfere with IFN induction and signaling (Sa Ribero et al., 2020). These immune evasion strategies are not well understood and require further elucidation.

Nanoparticles, or molecules less than 100 nm in diameter, are ideal candidates for carrying innate immune stimulants (Medina et al., 2007). In fact, nanoparticles of various compositions have shown promise as carriers of poly inosinic: poly cytidylic acid (pIC), a commercially available viral dsRNA mimic, while effectively stimulating the immune system (Kim et al., 2017; Sokolova et al., 2017; Gondan et al., 2018). Because nanoparticles of inorganic composition can have negative impacts on cells and their responses (Jeng and Swanson, 2006; Villeret et al., 2018; Báez et al., 2021; reviewed by Sengul and Asmatulu, 2020), optimization with an organic nanoparticle, such as the phytoglycogen nanoparticle (NDX) previously used by our group (Alkie et al., 2019; Jenik et al., 2021a; Jenik et al., 2021b), would be ideal. Previous work has shown that this phytoglycogen nanoparticle is non-toxic, can effectively deliver pIC to vertebrate cells, and can successfully limit

rhabdovirus replication (Alkie et al., 2019). Despite these promising results, the ability of pIC+NDX to limit HCoV replication is currently unkown.

Cell culture remains an essential tool within the toolbox of every virologist. This fundamental technique has been the source of many virological discoveries, such as understanding viral replication cycles, their interactions with host immunity and viral diagnostics. Indeed, following the discovery of any novel virus, a rapid search ensues to identify appropriate cell lines that can support replication and enable their study. Such has been the case for HCoVs as well (Kaye et al., 2006; Schildgen et al., 2006; de Wilde, 2013 and Pyrc et al., 2010). As an example, HCoV-HKU1 research was greatly hampered until a permissive cell line was identified (Pyrc et al., 2010). IFN-incompetent cell lines, such as the African green monkey kidney cell line Vero (Emeny and Morgan, 1979), are commonly used to study HCoVs, particularly MERS-CoV (de Wilde et al., 2013; Bracci et al., 2020). While excellent at propagating high titres of MERS-CoV, these cells are not appropriate for studying IFN-related interactions. Human lung cells with intact IFN pathways and the ability to support high levels of virus replication would be beneficial for furthering coronavirus research, particularly for understanding virus/host interactions at the cellular level.

The present study firstly investigates the permissiveness of HEL-299 cells to five HCoVs: HCoV-229E, -OC43, -NL63, MERS-CoV and SARS-CoV-2. Second, it investigates the ability of pIC+NDX to induce an IFN-mediated response in HEL-299 cells over time. The protective effect of this antiviral response was investigated with HCoV-229E, -OC43 and MERS-CoV. These data suggest that HEL-299 is a promising cell line for human coronavirus research and that dsRNA conjugated phytoglycogen nanoparticles hold promise, not only as tools for studying innate anti-coronavirus immune responses, but perhaps as future anti-coronavirus therapeutics.

2. Materials and methods

2.1. Cells

Two human embryonic lung cell lines, MRC-5 (ATCC, CCL-171) and HEL-299 (ATCC, CCL-137), were obtained from the American Type Culture Collection (ATCC). The MRC-5 cells were propagated in Eagle's minimum essential medium (EMEM) while the HEL-299 cells were cultured in Dulbecco's modified eagle medium (DMEM, Sigma). The liver hepatocellular carcinoma cell line, HepG2 (ATCC, HB-8065), was also cultured in EMEM. The human colonic epithelial cell line, HCT-8 (ATCC, CCL-244), was cultured in Roswell Park Memorial Institute (RPMI)-1640 medium (Corning). The media used for all of the above cell lines was supplemented with 10% fetal bovine serum (FBS, Seradigm) and 1% penicillin-streptomycin (P/S, Sigma). The green monkey kidney epithelial cell line, Vero (ATCC, CCL-81), was cultured in modified eagle medium (MEM) supplemented with 10% bovine growth serum (BGS), 1% P/S, and 2% L-glutamine (L-glut). VeroE6 cells (ATCC, CRL-1586) were cultured in DMEM (Hyclone) supplemented with 5% Bovine Growth Serum (Hyclone). All cells were grown in vented T75 flasks (BD Falcon) at 37°C with 5% CO_2.

2.2. Viruses

2.2.1. Propagation

Human coronavirus (HCoV)-229E (ATCC, VR-740), HCoV-OC43 (ATCC, VR-1558) and HCoV-NL63 (ATCC, VR-470) were obtained from the ATCC. MERS-CoV-GFP was generated using a reverse genetics system, as described previously (Nikiforuk et al., 2016). This virus was generated with GFP in place of MERS ORF5, and was grown on VeroE6 cells. SARS-CoV-2 (Canada/ON-VIDO-01/2020; EPI_ISL_425177) was isolated from a positive patient sample then grown and titered in VeroE6 cells.

HCoV-229E was propagated in MRC-5 cells that were grown in

vented T75 flasks. Briefly, MRC-5 cells were grown to 80% confluency. All normal growth media was removed and was replaced with 3 mL of serum-free EMEM. HCoV-229E was added to the cell monolayer. The infected flask was incubated at 33°C and 5% CO_2 for 2h with gentle rocking every 10 min. Following this incubation, 7 mL of EMEM containing 2% FBS was added to the flask. The cells were incubated at 33°C and 5% CO_2 for 3 days. The entire flask was frozen and thawed twice, thereafter the cell supernatant was collected and centrifuged at 10,000 x g for 10 min at 4°C. HCoV-OC43 was propagated in HCT-8 cells. Briefly, HCT-8 cells were grown to 80% confluency in vented T75 flasks. All of the normal growth media was removed and replaced with 3 mL of serum-free RPMI-1640. The flasks were then infected with HCoV-OC43 in serum free RPMI-1640 for 3h. Following this incubation, an additional 7 mL of RPMI-1640 containing 2% FBS was added. The cells were incubated at 33°C for 7 days with 5% CO_2. The entire flask was frozen and thawed three times, after which the cell supernatant was collected and centrifuged at 10,000 x g for 10 min at 4°C. After clearing the cellular debris, all cell supernatants were stored at -80°C for future use. HCoV-NL63 was not propagated but used directly from the vial received from ATCC.

2.2.2. Titration by tissue culture infectious dose (TCID$_{50}$)

The cell lines described above for viral propagation were seeded in 96-well plates (1.5×10^4 cells/well) and were used to titer their respective human coronaviruses by TCID$_{50}$. Following overnight adherence, all wells were washed once with basal media. For HCoV-229E and HCoV-OC43, supernatants of interest were serially diluted 1:10 in media containing 2% FBS. For each sample dilution, 100 µL was added to the 96-well plate in six-fold. Plates were then incubated at 33°C with 5% CO_2. At seven days post-infection (dpi), wells were scored by the presence of cytopathic effects (CPE). For MERS-CoV-GFP, supernatants were serially diluted in MEM containing 1% FBS, 1% P/S, and 2% L-Glutamine and 100 uL was added to triplicate wells in a 96 well plate format. Cells were incubated at 37°C with 5%CO_2 and CPE was scored on day 5 post-infection. Viral titers were calculated using the Reed and Meunsch method to obtain the TCID$_{50}$/mL (Reed and Muensch, 1938). Neither SARS-CoV-2 nor NL63 was titred as no CPE was observed.

2.3. Susceptibility of HEL-299 to human coronaviruses

To determine whether HEL-299 was permissive to different human coronaviruses, the cells were exposed to HCoV-229E, HCoV-OC43, HCoV-NL63, MERS-CoV-GFP, and SARS-CoV-2. HEL-299 cells were seeded into a 12-well plate (BD Falcon) at a density of 2.0×10^5 cells/well. The cells were allowed to adhere overnight before the monolayer was washed twice with media and infected with either HCoV-229E or HCoV-OC43 both at an MOI of 0.002, HCoV-NL63 at an MOI of 0.03, MERS-CoV-GFP at an MOI of 0.001, or SARS-CoV-2 at an MOI of 0.1, 0.01 and 0.001. HCoV-229E, HCoV-OC43, HCoV-NL63 infected plates were incubated at 33°C with 5% CO_2. MERS-CoV-GFP and SARS-CoV-2 infected cells were incubated at 37°C with 5% CO_2. On days 3 and 6, the cells were observed under an inverted microscope for CPE and cell supernatants were collected for virus titration as described above in Section 2.2.2.

2.4. Presence of the ACE2 receptor on HEL-299

2.4.1. ACE2 transcript levels by qRT-PCR

To determine whether HEL-299 contain the ACE2 gene, the expression of ACE2 mRNA was assessed. Total mRNA was extracted from a confluent T75 flask of HEL-299 cells (6.0×10^6 cells) and the positive control HepG2 cells (5.0×10^6 cells) using TRIzol Reagent (Invitrogen) as per the manufacturer's instructions. RNA was treated with Turbo DNA-free^{TM} kit (Invitrogen) to remove any contaminating genomic DNA. Complementary DNA (cDNA) was synthesized from 500 ng of purified RNA using the iScript^{TM} cDNA Synthesis Kit (Bio-Rad) following

protocols provided by the manufacturer.

The expression of ACE2 and the β-actin endogenous control was assessed via quantitative real-time polymerase chain reaction (qRT-PCR). All PCR reactions contained: 2 µL of 1:10 diluted cDNA, 2x SsoFast EvaGreen Supermix (Bio-Rad), 0.2 mM of forward primer (Sigma Aldrich), 0.2 mM of reverse primer (Sigma Aldrich) and nuclease-free water to a total volume of 10 µL (Fisher Scientific). The sequences and accession number for each primer set are outlined in Table 1. qRT-PCR reactions were performed using the CFX Connect Real-Time PCR Detection System (Bio-Rad). The program used for all qPCR reactions was: 98°C denaturation for 3 min, followed by 40 cycles of 98°C for 5 sec, 55°C for 10 sec, and 95°C for 10 sec. A melting curve was completed from 65°C to 95°C with a read every 5 sec. Product specificity was determined through single PCR melting peaks. The data is presented as the average C_t values of three experimental replicates with the standard error of the mean (SEM).

2.4.2. ACE2 immunocytochemistry (ICC)

To confirm the presence of known known human coronavirus receptors at the protein level, ICC was completed on HEL-299 for ACE2. One sterile, circular glass coverslip was placed in each well of a 12-well tissue culture plate. HEL-299 cells were then seeded at a density of 2.0×10^5 cells/well in basal media and allowed to adhere to the coverslips overnight at 37°C with 5% CO2. The positive control cells of HepG2 cells were seeded at a density of 2.0×10^4 cells/well.

Following overnight adherence, media was removed from each well and cells were washed once with DPBS. Cells were then fixed to coverslips with 10% neutral buffered formalin and incubated for 10 min at room temperature. Wells were washed three times and blocked overnight at 4°C with fresh ICC blocking solution (3% w/v BSA, 3% v/v goat serum, 0.02% v/v Tween-20). Wells were washed once with DPBS and incubated for 1h in a humidified chamber with a 1:100 dilution of ACE2 recombinant rabbit monoclonal antibody (ThermoFisher, Cat No. MA5-32307). Wells were washed three times with DPBS before being incubated with a 1:200 dilution of goat anti-rabbit Alexa Fluor plus 488 secondary antibody (ThermoFisher, Cat No. A32731) in a humidified chamber for 1h in the dark. All wells were washed three times with DPBS. The cellular nuclei were stained using 5 µg/mL of DAPI and incubated in the dark for 5 min. Wells were washed three times with DPBS and once with milliQ water to remove residual salt. Coverslips were mounted on glass microscope slides using 3 µL of SlowFade Gold Antifade mountant. For negative control wells, cells were probed with only the secondary antibody to ensure that non-specific binding was not occurring.

2.5. Nanoparticle and pIC formulations

A commercial grade phytoglycogen nanoparticle (NanoDendrix™ (NDX), Glysantis, Guelph, ON, Canada) derived from sweet corn was modified to attain a net positive surface charge, herein referred to as

Table 1

The qRT-PCR primer sequences used to measure human antiviral gene expression and the ACE2 HCoV receptor. Forward (F) and reverse (R) primers are provided as well as the reference or genbank accession number for each gene.

Primer	Sequence (5'-3')	Reference or Accession No.
IFNβ	**F:** AAACTCATGAGCAGTCTGCA	Semple et al., 2022
	R: AGGAGATCTTCAGTTTCGGAGG	
CXCL10	**F:** GAAAGCAGTTAGCAAGGAAAGG	Semple et al., 2022
	R: GACATATACTCCATGTAGGGAAGTG	
ISG15	**F:** CAGCCATGGGCTGGGAC	NM_005101.4
	R: CTTCAGCTCTGACACCGACA	
ACE2	**F:** GGCTCCTTCTCAGCCTTGTT	LC698008.1
	R: GGTCTTCGGCTTCGTGGTTA	
β-Actin	**F:** CTGGCACCCAGCACAATG	Semple et al., 2022
	R: CCGATCCACACGGAGTACTTG	

cationic phytoglycogen nanoparticles (Ph-NPs). Both the nanoparticles and the synthetic dsRNA analogue, called High Molecular Weight (HMW) poly(I:C) (pIC, InvivoGen) were re-suspended at 1 mg/mL in nuclease free water. The pIC and cationic Ph-NPs were mixed by gentle pipetting at 1:1 ratio and incubated at room temperature for 30 minutes for the formation of pIC-Ph-NPs complexes through simple electrostatic interactions between the negatively charged pIC and the cationic Ph-NPs. The physical properties of the dsRNA and nanoparticles were characterized as described previously (Alkie et al., 2019). In the present study, the pIC-Ph-NPs complex is designated as pIC+NDX. The HMW poly(I:C) is denoted as pIC. The cationic Ph-NPs alone are designated as NDX.

2.6. Viability of HEL-299 cells to pIC and NDX treatments

To assess whether the pIC and NDX formulations influenced the survival of HEL-299, two fluorescent indicator dyes, alamarBlue (AB, Invitrogen) and 5-carboxyfluorescein diacetate acetoxymethyl ester (CFDA-AM, Invitrogen), were used. Together these dyes provide an excellent indication of cell viability as both cellular metabolism (AB) and membrane integrity (CFDA-AM) are measured (Dayeh et al., 2003). HEL-299 cells were seeded at a density of 2.0×10^4 cells/well in a 96-well tissue culture plate and allowed to adhere overnight at 37°C with 5% CO_2. All cell monolayers were washed twice with media and then treated in six replicate wells with either 1 µg/mL pIC+NDX, 1 µg/mL NDX, 1 µg/mL pIC, or media alone for 24h at 37°C with 5% CO_2. Following incubation, each well was washed twice with PBS before exposure to AB and CFDA-AM as described by Dayeh et al. (2003). Plates were read on a Synergy HT plate read as outlined previously by Semple et al. (2022). Results are presented as a percentage of untreated control cells and represents the average of at least 3 independent experiments.

2.7. Induction of antiviral genes following stimulation of HEL-299 cells with pIC and NDX

2.7.1. RNA extraction and cDNA synthesis

To determine the impact of pIC and NDX conjugates on innate antiviral gene stimulation, HEL-299 cells were seeded (2×10^5 cells/well) in 12-well cell culture plates and incubated for 24 h at 37°C with 5% CO_2. The cell monolayer was washed twice with media and then treated with either 1 µg/mL pIC+NDX, 1 µg/mL NDX or 1 µg/mL pIC for 6, 24, 48, 72 and 168h. The dose of 1 µg/mL pIC was selected after a dose response curve was performed looking at IFN production and 1 µg/mL pIC demonstrated the greatest difference between pIC and pIC+NDX (data not shown). Control groups received media alone. Total RNA was extracted and cDNA synthesized as described above in Section 2.4.1.

2.7.2. qRT-PCR

The expression of antiviral immune genes (IFNβ, CXCL10 and ISG15) was measured by qRT-PCR as described above in Section 2.4.1 with the sequences and accession number for each primer set outlined in Table 1. All qRT-PCR data was analyzed using the $\Delta\Delta C_t$ method and is presented as the average of three experimental replicates with the standard error of the mean (SEM). Specifically, gene expression was normalized to the housekeeping gene (β-actin) and presented as fold changes over the control group.

2.8. Inhibition of HCoV infections of HEL-299 following pre-stimulation with pIC and NDX

2.8.1. HCoV-229E and HCoV-OC43

HEL-299 cells were seeded in 12-well plates at a density of 2.0×10^5 cells/well in DMEM and were allowed to adhere overnight. Cells were washed twice with PBS and treated with either 1 µg/mL of pIC, 1 µg/mL of NDX, 1 µg/mL of pIC+NDX or basal media alone and incubated at 37°C with 5% CO_2. At either 6 or 24h post-exposure, the media was

supplemented with 2% FBS and the cell monolayers were infected with HCoV-229E or HCoV-OC43 at a MOI of 0.002. An untreated, uninfected cell control was included. Plates were then incubated at 33°C with 5% CO_2. At 1, 2, 3, 4 and 7 dpi, all plates went through two to three freeze-thaw cycles, after which the cell supernatant was collected and centrifuged at 10,000 x g for 10 min at 4°C. Supernatants were stored at -80°C until the $TCID_{50}$ assay could be performed as described above in Section 2.2.2. Microscopic images were taken of each well at all time points to document the appearances of CPE.

2.8.2. HCoV-MERS-GFP

HEL-299 cells were seeded in 12-well plates at a density of 2.0×10^5 cells/well in basal MEM media and allowed to adhere overnight. Cells were exposed to the same treatments as described in Section 2.8.1 for 24h, after which the media was supplemented with BGS to a final concentration of 2%. MERS-CoV-GFP was then added to the cells at either an MOI of 0.01 or 0.001. All wells included in each experiment were run in triplicate and supernatants from each well were collected on days 2, 4, and 6h post-infection. Supernatants were stored at -80°C until a $TCID_{50}$ assay was performed as described above in Section 2.2.2. Additionally, microscopic images were taken of each well on days 2, 4, and 6 to document any CPE from infection. Untreated, uninfected media control wells were included on each plate for reference.

2.9. Statistical analyses

All data sets were tested for a normal distribution (Shapiro-Wilk) and homogeneity of variance (Levene's) using R (R Core Team, 2014; RStudio Team, 2015). Further statistical analyses were competed with GraphPad (Version 8, GraphPad, La Jolla, CA). A one-way analysis of variance (ANOVA) was competed to compare mean between treatment groups, followed by a Tukey's post-hoc test for gene expression and viral titers) or a Dunnett's post-hoc test for (viability data). Data is presented as the average of experimental replicates with the SEM. A p-value of $p \leq 0.05$ was considered statistically significant.

3. Results

3.1. HEL-299 is permissive to HCoV-229E, -OC43 and MERS-CoV-GFP

When HEL-299 cells were exposed to either HCoV-229E, HCoV-OC43, HCoV-NL63, MERS-CoV-GFP or SARS-CoV-2, the human lung fibroblasts demonstrated CPE with three of these viruses (Fig. 1). When compared to control uninfected cells (Fig. 1A), significant CPEs were observed in cells exposed to HCoV-229E (Fig. 1B), HCoV-OC43 (Fig. 1C) and MERS-CoV-GFP (Fig. 1E) at 5 dpi. In comparison, infection with HCoV-NL63 and SARS-CoV-2 resulted in no changes to cellular morphology (Figs. 1D and F) indicating that HEL-299 is likely not permissive and/or susceptible to these viruses.

3.2. The ACE2 receptor is absent in HEL-299 cells

Both HCoV-NL63 and SARS-CoV-2 require the ACE2 receptor to attach/enter host cells and these viruses were unable to infect HEL-299. As a result, the presence of the ACE2 receptor was explored in HEL-299. At the transcript level, HEL-299 did not have detectable levels of ACE2 mRNA while the HepG2 positive control cells did present amplification of this transcript (Fig. 2A). When ACE2 presence was further assessed at the protein level by ICC, HEL-299 did not contain ACE2 protein (Fig. 2Bi), but was detectable in the positive control HepG2 cells (Fig. 2Bii). At both the transcript and protein level, HEL-299 is not positive for the ACE2 receptor (Fig. 2).

3.3. PIC and NDX formulations influence HEL-299 cellular metabolism

In order to explore the impact that pIC and pIC+NDX conjugates had
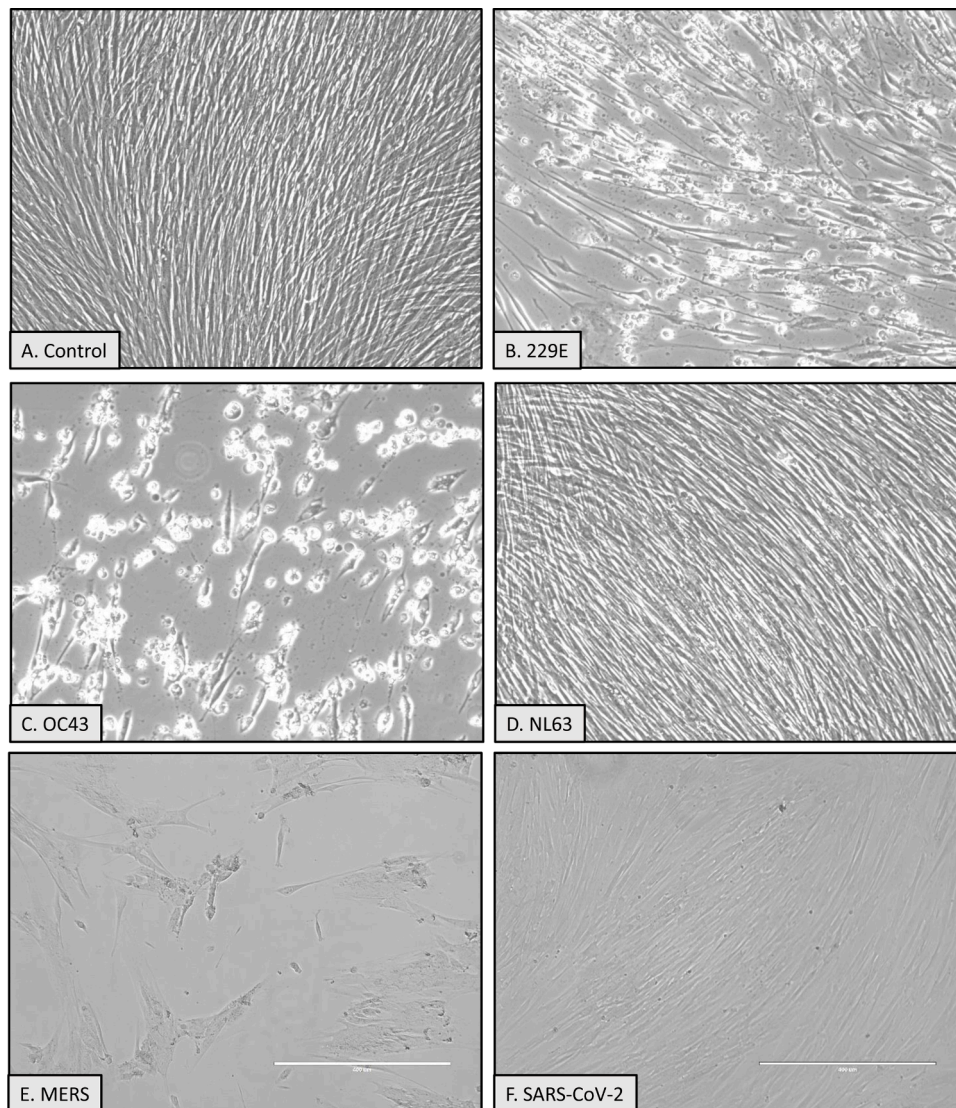
Fig. 1. Permissiveness of HEL-299 cells to human coronaviruses. Following exposure to five different human coronaviruses, microscopic images of HEL-299 cells were taken at 5 days post-infection (100x). The HEL-299 cells were exposed to media alone to act as an uninfected control (**A**) or infected with, HCoV-229E (**B**), HCoV-OC43 (**C**), HCoV-NL63 (**D**), MERS-CoV-GFP (**E**) and SARS-CoV-2 (**F**).

on IFN mediated, anti-HCoV responses, it was first necessary to ensure that the pIC and NDX formulations were not themselves negatively impacting HEL-299 viability. Following a 24h exposure to the pIC and NDX preparations, HEL-299 cells treated with the pIC+NDX complex were observed to have a reduction in cellular metabolism when compared to untreated cells as indicated by the Alamar Blue assay (Fig. 3A, Control = 100% ± 0% SEM, NDX = 89.76% ± 4.71% SEM, pIC = 85.17% ± 6.31% SEM and pIC+NDX = 63.35% ± 4.50% SEM). However, cellular membrane integrity, as measured using CFDA-AM, was unaffected in any treatment group (Fig. 3B). When microscopic images were taken following the 24h treatments there were no obvious differences in cellular morphology between groups (Fig. 3C).

3.4. PIC and NDX complexes induce stronger antiviral immune responses in HEL-299 cells

The ability of pIC and NDX formulations to induce IFN pathways was then tested. After HEL-299 cells were stimulated with pIC and NDX formulations for 6, 24, 48 and 168h, differences in antiviral gene expression (IFNβ, CXCL10 and ISG15) were observed. Administration of pIC alone was only able to induce significant upregulation of IFNβ and

CXCL10 at 6h post-stimulation, otherwise gene expression in this group did not differ from the untreated controls (Fig. 4). In comparison, the complex of pIC+NDX induced significant upregulation of all three antiviral genes at 6h post-exposure when compared to the control and was significantly higher than pIC alone for IFNβ and CXCL10 expression at this time point (Fig. 4A). Furthermore, treatment with the pIC+NDX complex resulted in significant upregulation of IFNβ and CXCL10 at 24 and 168h post-stimulation (Figs. 4Bi-ii and Di-ii), but ISG15 expression was only significantly upregulated in this group at 168h (Figs. 4Biii and Diii). For all treatments, antiviral gene expression did not differ from the control at 48h post-stimulation (Fig. 4C). The NDX alone treatment did not induce any gene expression and results remained similar to the control untreated groups at all time points (Fig. 4).

3.5. PIC and NDX complexes inhibited HCoV replication in HEL-299 cells

Pre-treatment of HEL-299 cells with pIC for 6h induced a significant reduction in HCoV-229E titers at 1 and 2 dpi (Fig. 5Ai) and that of HCoV-OC43 titers at 1, 2 and 4 dpi (Fig. 5Bi) compared to untreated infected controls. When HEL-299 was pre-treated for 6h with pIC+NDX complexes, viral production was not observed at all until 7 dpi for both

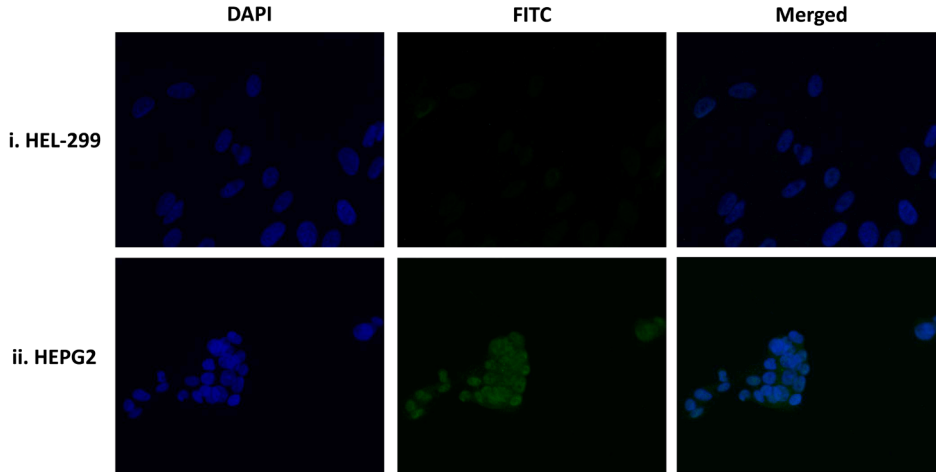## A. ACE2 Transcript
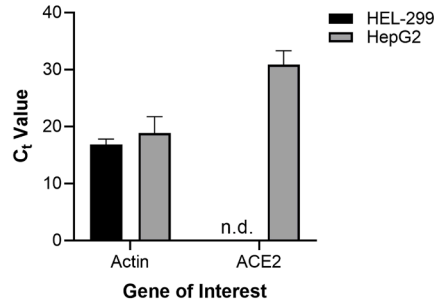
B. ACE2 ICC

Fig. 2. The ACE2 receptor is absent in HEL-299 cells. Following mRNA extraction from HEL-299 and the positive control HepG2 cell line, C_t values for ACE2 and the β-actin endogenous control were reported via qRT-PCR analysis (**A**). At the protein level, immunocytochemistry (ICC) was completed on HEL-299 cells to probe for the ACE2 receptor (**Bi**). This ICC was also completed on the positive control HepG2 cell line as these cells are known to contain the ACE2 receptor (**Bii**). Both cell types were formalin fixed to glass coverslips and nuclei were stained with DAPI following probing with the rabbit anti-ACE2 antibody. All data represents three independent replicates.

A. Alamar Blue
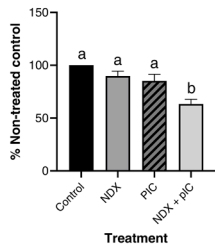
B. CFDA

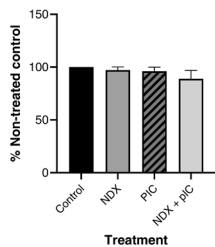## C. Representative Images (24h)
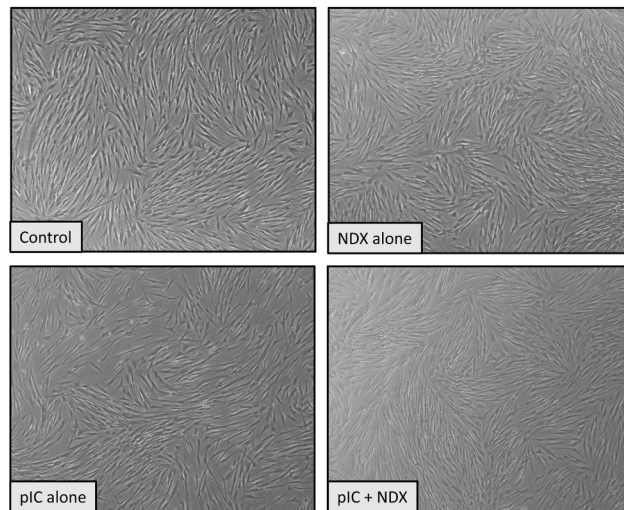
Fig. 3. Viability of HEL-299 when treated with pIC and NDX formulations. Following 24h exposure to the pIC and NDX treatments, the fluorescent indicator dyes alamarBlue and CFDA-AM were used to measure HEL-299 cell viability. Assessment of cellular metabolism (**A**) and membrane integrity (**B**) is presented. All data was displayed as the percent relative fluorescent units (RFUs) of the untreated control. The data presented in these panels represents six independent experiments and is presented as the mean + SEM. Following a one-way ANOVA and Dunnett's post-hoc test, a p-value of less than 0.05 was considered to be statistically significant when compared to the unstimulated control for each timepoint. Error bars with different letters represent significantly different data. Microscopic images of the HEL-299 cells following 24h exposure to each treatment condition are also presented at 40x magnification (**C**).

HCoV-229E and HCoV-OC43 (Fig. 5Ai and Bi). Following pre-treatment for 24h, pIC alone displayed a similar inhibitory pattern to what was observed at the 6h pre-treatment condition wherein viral titers were significantly reduced for HCoV-229E at 1 and 2 dpi (Fig. 5Aii) and HCoV-OC43 at 1, 2 and 3 dpi (Fig. 5Bii). In comparison, the inhibition observed after 6h pre-treatment with pIC+NDX was strengthened when HEL-299 cells were pre-treated for the longer duration of 24h. In the 24h

pre-exposure of pIC+NDX, both HCoV-229E and HCoV-OC43 viral titers were undetectable at all timepoints, up to 7 dpi (Figs. 5Aii and Bii). Regardless of the virus and in either of the pre-treatment conditions, NDX alone did not significantly differ from the untreated control condition at all of the timepoints studied (Fig. 5).

Twenty-four hour pre-treatment with the pIC and NDX formulations was also able provide protection to HEL-299 against MERS-CoV-GFP
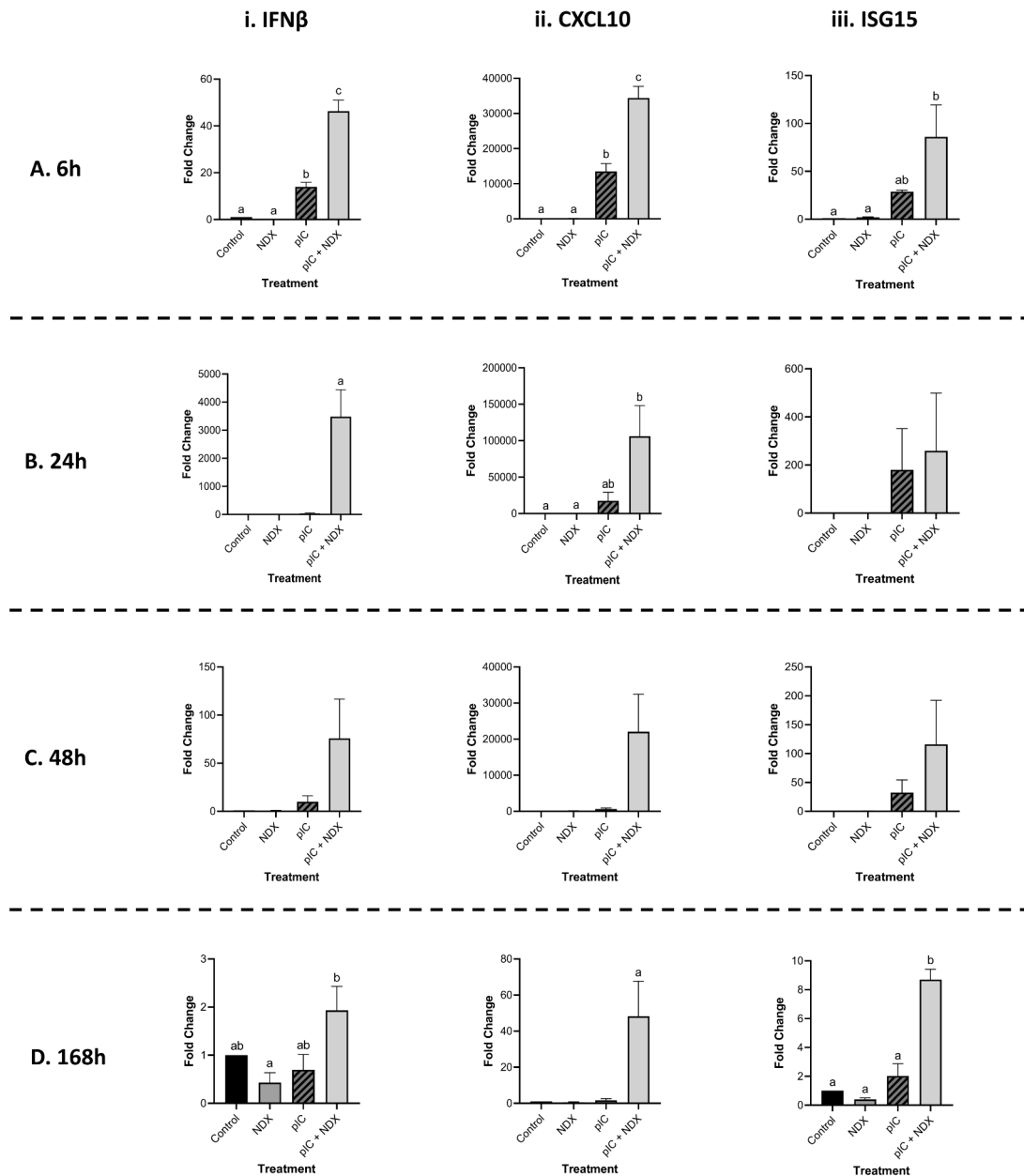
Fig. 4. Treatment with pIC and NDX conjugates induces potent antiviral gene expression. HEL-299 cells were exposed to pIC alone, NDX alone, pIC+NDX and a media only control so that gene expression could be analyzed at 6h (**A**), 24h (**B**), 48h (**C**) and 168h (**D**). The antiviral immune genes of interest were IFNβ (**i**), CXCL10 (**ii**) and ISG15 (**iii**). These genes were normalized to β-actin and presented as the fold change relative to the unstimulated control. All panels represent three independent experiments and are presented as means + SEM. Following a one-way ANOVA and Tukey's post-hoc test, a p-value of less than 0.05 was considered to be statistically significant when compared to the unstimulated control for each timepoint. Error bars with different letters represent significantly different data.

(Fig. 6). At an MOI of 0.01, pre-treatment with pIC+NDX significantly reduced the viral titer at 2 dpi, but this inhibition was lost by 4 dpi (Fig. 6A). At all other timepoints as well as in the pIC alone treatment, viral titers were not significantly different from the untreated control (Fig. 6A). Following exposure of HEL-299 to MERS-CoV-GFP at an MOI of 0.001, only the pIC+NDX treatment at 2 dpi was significantly different from the unexposed control (Fig. 6B). In this condition, the pIC alone treatment was not significantly different from either the control or the pIC+NDX treatment. At all other timepoints, none of the treatment conditions stimulated significant inhibition of the virus when compared to the control (Fig. 6B). Additionally, a 6h pre-treatment with pIC and NDx formulations provided no protection to HEL-299 against MERS-CoV-GFP (data not shown).

4. Discussion

Cell lines are an important tool for studying virus replication *in vitro*. Of the five HCoVs that were tested in this study, HEL-299 cells were able to support the replication of HCoV-229E, -OC43 and MERS-CoV to higher titers. Most HCoV studies use either MRC5 or HCT-8 cells for propagating HCoV-229E and -OC43 respectively, while Vero cells are used for the growth of MERS-CoV (Funk et al., 2012; Coleman and Frieman, 2015; Warnes et al., 2015; Owczarek et al., 2018). The permissiveness of HEL-299 cells to HCoV-229E and -OC43 but not SARS-1 (Kaye et al., 2006; Persoons et al., 2021) has been reported previously. However, the ability of this cell line to support MERS-CoV replication as well as its inability to perpetuate SARS-CoV-2 and
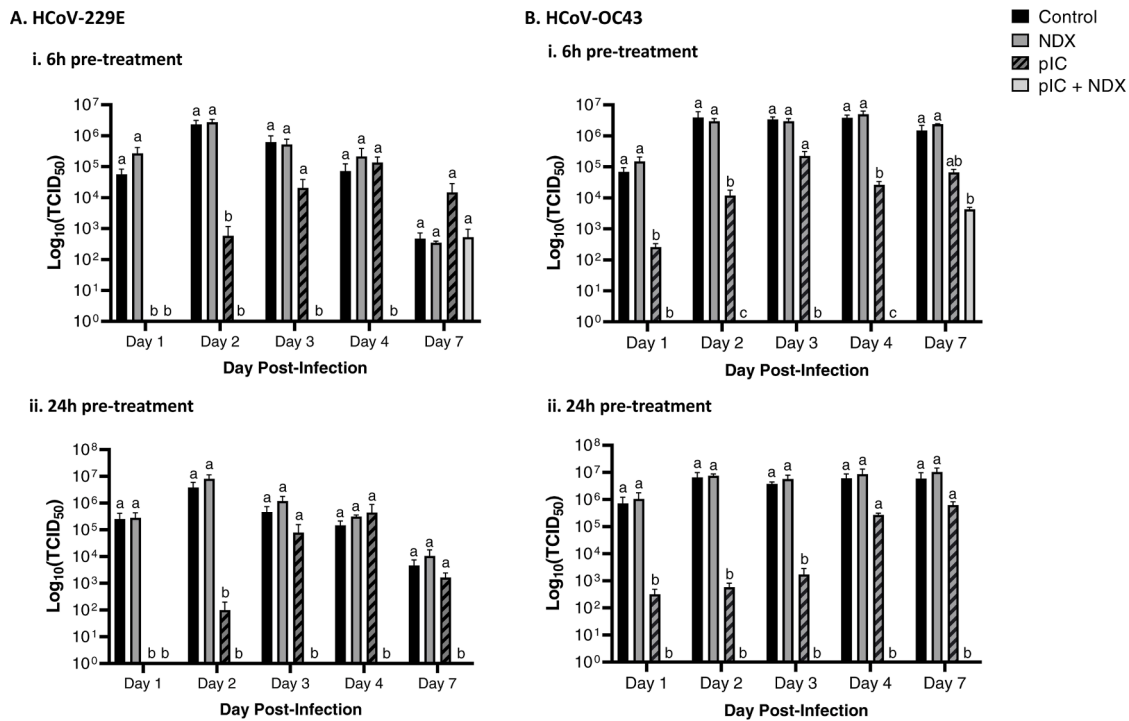
Fig. 5. Pre-treatment with pIC and NDX formulations can protect HEL-299 from HCoV-229E and HCoV-OC43. HEL-299 cells were infected with HCoV-229E (**A**) and HCoV-OC43 (**B**) (MOI = 0.002) following either 6h (**i**) or 24h (**ii**) pre-stimulation with either media only (control), pIC alone, NDX alone or pIC+NDX. Each panel represents three independent experiments and is presented as the mean + SEM. Following a two-way ANOVA and Tukey's post-hoc test, a p-value of less than 0.05 was considered to be statistically significant when data was compared at each timepoint. Error bars with different letters represent significantly different data within the same timepoint.
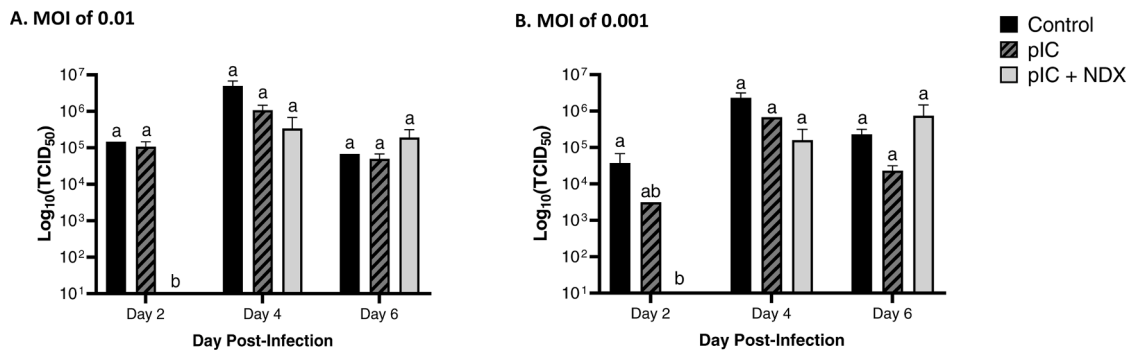
Fig. 6. MERS-CoV-GFP infection can be inhibited via pre-treatment with pIC and NDX conjugates. After 24h pre-exposure with either media only (control), pIC alone, NDX alone or pIC+NDX, HEL-299 cells were infected with MERS-CoV-GFP at an MOI of 0.01 (**A**) or 0.001 (**B**). Each panel represents three independent experiments and is presented as the mean + SEM. Following a two-way ANOVA and Tukey's post-hoc test, a p-value of less than 0.05 was considered to be statistically significant when data was compared at each timepoint. Error bars with different letters represent significantly different data within the same timepoint.

HCoV-NL63 infection is novel. Given the pattern of HCoV propagation observed here, it would be anticipated that HEL-299 cells have CD13, 9-O-Ac-Sia and CD26 receptors (reviewed by Guruprasad, 2021) while lacking the ACE2 receptor required for SARS-CoV-2 and HCoV-NL63 infection (Milewska et al., 2014; reviewed by Scialo et al., 2020). Indeed, when explored further, the ACE2 receptor was not observed at both the transcript and protein level in HEL-299. Additionally, because the Vero cells typically used for MERS-CoV propagation are not IFN competent (Emeny and Morgan, 1979), the IFN competent HEL-299 cells could provide a considerable improvement for understanding the immune response to this virus. When compared to other permissive human cell lines, HEL-299 cells were able to stimulate MERS-CoV titers greater than 10^6 TCID$_{50}$/mL after 4 dpi, making this cell line comparable to VeroE6 cells which produce similar titres at 40 hpi (Eckerle et al.,

2014). Having an alternative cell line that is both lung-derived and has an intact IFN response will be valuable for MERS-CoV research, particularly for studying host-virus interactions.

After evaluating the permissiveness of HEL-299 to HCoVs, the antiviral effects of pIC either alone or conjugated to a phytoglycogen nanoparticle (NDX) was tested. Nanoparticles have gained a great deal of attention for their ability to deliver pharmaceuticals and therapeutic compounds (reviewed in Chakravarty and Vora, 2021); however, the potential cytotoxic effects associated with most inorganic nanoparticles have warranted the need to examine safer alternatives (reviewed in Sengul and Asmatulu, 2020). In the present study, while the cellular metabolism of HEL-299 cells were reduced upon treatment with pIC+NDX, cell membrane integrity remained unaffected. Previous studies documented that pIC can cause a reduction in cellular

metabolism by inducing an antiviral state (reviewed in Fritsch and Weichhart, 2016), thus CFDA-AM may be a better indicator of cell viability in this situation. Additionally, the cell monolayers appeared healthy as determined by microscopy, providing further support that the NDX was not cytotoxic.

A key component of innate antiviral immunity is the ability of IFNs to stimulate the production of ISGs, as these effector proteins accumulate to form an antiviral state within the cell (reviewed by Yang and Li, 2020). The robust production of IFN and associated ISGs is critical for the successful prevention of viral infections. This has been previously shown by Lenschow and colleagues (2007) when ISG15 knockout mice were found to be more susceptible to various strains of influenza, herpes simplex and Sindbis viruses when compared to their functional ISG15 counterparts. Our group and others have shown that pIC complexed with nanoparticles are superior to pIC in inducing an antiviral state through the production of IFNs and ISGs in large vertebrate models and in aquatic species (Kim et al., 2017; Sokolova et al., 2017; Speth et al., 2017, Alkie et al., 2019). The results presented here demonstrate that delivering pIC complexed with NDX induced a stronger type I IFN response in IFN competent human lung fibroblasts (HEL) when compared to pIC alone. Moreover, the same formulation induced ISGs until 168h post-stimulation suggesting a more stable IFN-induction platform over time. Thus, pIC induced IFN responses were strong and longer-lasting using NDX. This is likely due to NDX mediated receptor clustering and stabilizing dsRNA degradation (Alkie et al., 2019). The potent production of IFNs and ISGs by pIC+NDX could provide a unique perspective for studying the effects of IFNs in modulating HCoV replication over time and ultimately preventing successful viral infection within the host cell.

Coronaviruses are known to modulate the host IFN response. For example, SARS-CoV-2 limits antiviral cytokine production *in vivo* (Kouwaki et al., 2021) and is known to produce at least 10 proteins that can influence type I IFN responses (Sa Ribero et al., 2020). Additionally, MERS-CoV evades host immunity not only by suppressing type I IFN pathways, but by also by introducing repressive histone modifications to decrease the expression of ISG subsets (Menachery et al., 2014). Despite all of these immune-evasion mechanisms, inducing or administering IFNs at or prior to infection can suppress viral replication. This was observed when type I IFNs were administered during the early stages of COVID-19 infections resulting in reduced patient mortality (Park and Iwasaki, 2020; Davoudi-Monfared et al., 2020; Wang et al., 2020) and this treatment has also been shown to inhibit SARS-CoV-2 infection in various *in vitro* models (Felgenhauer et al., 2020; Vanderheiden et al., 2020). Additionally, early treatment with pIC alone has been shown stimulate protection against SARS-CoV-1 and MERS-CoV in mouse models (Zhao et al., 2012; Wang et al., 2017). In the present study, pIC+NDX treatment resulted in enhanced antiviral responses and protected against HCoV infection when compared to pIC alone. The pre-treatment with pIC alone was observed to significantly delay infection of HEL with HCoV-229E and -OC43. Interestingly, when pIC was conjugated to the NDX nanoparticle and then used for pre-treatment, infection with all three of the HCoVs investigated were either significantly delayed further than what was observed with pIC alone or completely prevented. Using pIC and NDX nanoparticle complexes to induce a potent, and early, antiviral IFN response is one method to significantly inhibit or completely stop the infection of HCoVs in permissive cell lines. This IFN-induction capacity holds value for future studies *in vivo*. Indeed, pIC-loaded calcium phosphate nanoparticles coated with liver targeted antibodies demonstrated significant uptake in murine livers resulting in protection against hepatitis B viral infection (Du et al., 2021). Thus, furthering our understanding of pIC conjugated to NDX could help develop a very interesting tool for studying HCoV-host interactions in animals models and holds potential as a new avenue for antiviral therapies, pending further analysis and toxicity testing *in vivo*.

The results of the present study introduce new tools for studying

HCoVs, particularly within the context of type I IFN signaling. HEL-299, as an IFN-competent, human lung cell line may prove to be an important model system to study HCoV-host interactions as they relate to IFNs. Additionally, as a potent inducer of IFNs over time, use of pIC+NDX is an excellent system for understanding the temporal effects of IFN on HCoV infections, *in vitro* and in future *in vivo* studies. These tools will aid in our fundamental understanding of human coronaviruses and how they interact with the cellular innate antiviral immune response, which is of utmost importance given the current HCoV pandemic.

CRediT authorship contribution statement

Shawna L Semple: Methodology, Validation, Formal analysis, Investigation, Writing – original draft, Writing – review & editing, Visualization. **Tamiru N Alkie:** Conceptualization, Methodology, Validation, Writing – original draft, Writing – review & editing. **Kristof Jenik:** Validation, Investigation. **Bryce M Warner:** Validation, Investigation, Formal analysis. **Nikesh Tailor:** Investigation. **Darwyn Kobasa:** Validation, Resources, Supervision, Funding acquisition. **Stephanie J DeWitte-Orr:** Resources, Writing – original draft, Writing – review & editing, Supervision, Project administration, Funding acquisition.

Declaration of Competing Interests

The authors declare that they have no known competing financial interests or personal relationships that could have appeared to influence the work reported in this paper.

Data availability

Data will be made available on request.

References

Alkie, TN, de Jong, J, Jenik, K, Klinger, KM, DeWitte-Orr, SJ, 2019. Enhancing innate antiviral immune responses in rainbow trout by double stranded RNA delivered with cationic phytoglycogen nanoparticles. Sci. Rep. https://doi.org/10.1038/s41598-019-49931-2.

Almeida, JD, Tyrrell, DA, 1967. The morphology of three previously uncharacterized human respiratory viruses that grow in organ culture. J. Gen. Virol. 1, 175–178.

Báez, DF, Gallardo-Toledo, E, Oyarzún, MP, Araya, E, Kogan, MJ, 2021. The influence of size and chemical composition of silver and gold nanoparticles on in vivo toxicity with potential applications to central nervous system diseases. Int. J. Nanomed. 16, 2187–2201.

Borden, EC, Sen, GC, Uze, G, Silverman, RH, Ransohoff, RM, Foster, GR, Stark, GR, 2007. Interferons at age 50: past, current and future impact on biomedicine. Nat. Rev. Drug Discovery 6, 975–990.

Bracci, N, Pan, H-C, Lehman, C, Kehn-Hall, K, Lin, S-C, 2020. Improved plaque assay for human coronaviruses 229E and OC43. PeerJ. https://doi.org/10.7717/peerj.10639.

Brennan, K, Bowie, AG, 2010. Activation of host pattern recognition receptors by viruses. Curr. Opin. Microbiol. 13, 503–507.

Coleman, CM, Frieman, MB, 2015. Growth and quantification of MERS-CoV infection. Curr Protoc Microbiol 37, 1521–1529.

Chakravarty, M, Vora, A, 2021. Nanotechnology-based antiviral therapeutics. Drug Deliv Transl Res 11, 748–787.

Chen, Y, Liu, Q, Guo, D, 2020. Emerging coronaviruses: genome structure, replication, and pathogenesis. J. Med. Virol. 92, 418–423.

Christian, MD, Poutanen, SM, Loutfy, MR, Muller, MP, Low, DE, 2004. Severe acute respiratory syndrome. Clin. Infect. Dis. 38, 1420–1427.

Chu, H, Chan, JF-W, Wang, Y, Yuen, TT-T, Chai, Y, Hou, Y, et al., 2020. Comparative replication and immune activation profiles of SARS-CoV-2 and SARS-CoV in human lungs: an ex vivo study with implications for the pathogenesis of COVID-19. Clin. Infect. Dis. https://doi.org/10.1093/cid/ciaa410.

Dayeh, VR, Schirmer, K, Lee, LEJ, Bols, NC, 2003. The use of fish-derived cell lines for investigation of environmental contaminants. Current Protocols in Toxicology. https://doi.org/10.1002/0471140856.tx0105s15.

da Costa, VG, Moreli, ML, Saivish, MV, 2020. The emergence of SARS, MERS and novel SARS-2 coronaviruses in the 21st century. Arch. Virol 165, 1517–1526.

Davoudi-Monfared, E, Rahmani, H, Khalili, H, Hajiabdolbaghi, M, Salehi, M, Abbasian, L, et al., 2020. A randomized clinical trial of the efficacy and safety of interferon β-1a in treatment of severe COVID-19. Antimicrob. Agents Chemother. https://doi.org/10.1128/AAC.01061-20.

de Wilde, AH, Raj, VS, Oudshoorn, D, Bestebroer, TM, van Nieuwkoop, S, Limpens, RWAL, et al., 2013. MERS-coronavirus replication induces severe in vitro cytopathology and is strongly inhibited by cyclosporin A or interferon-α treatment. J. Gen. Virol. 94, 1749–1760.

Du, Y, Yang, X, Li, J, Sokolova, V, Zou, S, Han, M, et al., 2021. Delivery of toll-like receptor 3 ligand poly(I:C) to liver by calcium phosphate nanoparticles conjugated with an F4/80 antibody exerts an anti-hepatitis B virus effect in a mouse model. Acta Biomater. 133, 297–307.

Eckerle, I, Corman, VM, Müller, MA, Lenk, M, Ulrich, RG, Drosten, C, 2014. Replicative capacity of MERS coronavirus in livestock cell lines. Emerg. Infect. Dis. https://doi.org/10.3201/eid2002.131182.

Emeny, JM, Morgan, MJ, 1979. Regulation of the interferon system: evidence that Vero cells have a genetic defect in interferon production. J. Gen. Virol. https://doi.org/10.1099/0022-1317-43-1-247.

Felgenhauer, U, Schoen, A, Gad, HH, Hartmann, R, Schaubmar, AR, Failing, K, et al., 2020. Inhibition of SARS-CoV-2 by type I and type III interferons. J. Biol. Chem. https://doi.org/10.1074/jbc.AC120.013788.

Fritsch, SD, Weichhart, T, 2016. Effects of interferons and viruses on metabolism. Front. Immunol. https://doi.org/10.3389/fimmu.2016.00630.

Funk, CJ, Wang, J, Ito, Y, Travanty, EA, Voelker, DR, Holmes, KV, et al., 2012. Infection of human alveolar macrophages by human coronavirus strain 229E. J. Gen. Virol. 93, 494–503.

Gondan, AIB, Ruiz-de-Angulo, A, Zableta, A, Blanco, NG, Sobaleda-Siles, BM, Garcia-Granda, MJ, 2018. Effective cancer immunotherapy in mice by polyIC-imiquimod complexes and engineered magnetic nanoparticles. Biomaterials 170, 95–115.

Guruprasad, L, 2021. Human coronavirus spike protein-host receptor recognition. Prog. Biophys. Mol. Biol. 161, 39–53.

Hagemeijer, MC, Vonk, AM, Monastyrska, I, Rottier, PJM, de Haan, CAM, 2012. Visualizing coronavirus RNA synthesis in time by using click chemistry. J. Virol. https://doi.org/10.1128/JVI.07207-11.

Hamre, D, Procknow, JJ, 1966. A new virus isolated from the human respiratory tract. Proc. Soc. Exp. Biol. Med. 121, 190–193.

Hu, B, Guo, H, Zhou, P, Shi, Z-L, 2020. Characteristics of SARS-CoV-2 and COVID-19. Nat. Rev. Microbiol. 19, 141–154.

Hulswit, RJG, Lang, Y, Bakkers, MJG, Li, W, Li, Z, Schouten, A, et al., 2019. Human coronaviruses OC43 and HKU1 bind to 9-O-acetylated sialic acids via a conserved receptor-binding site in spike protein domain A. Proc. Natl Acad. Sci. 116, 2681–2690.

Jeng, HA, Swanson, J, 2006. Toxicity of metal oxide nanoparticles in mammalian cells. J. Environ. Sci. Health A 41, 2699–2711.

Jenik, K, Alkie, TN, Moore, E, Dejong, JD, Lee, LEJ, DeWitte-Orr, SJ, 2021a. Characterization of a bovine intestinal myofibroblast cell line and stimulation using phytoglycogen-based nanoparticles bound to inosine monophosphate. In Vitro Cell. Dev. Biol. Anim. 57, 86–94.

Jenik, K, Alkie, TN, Samms, K, Lalousis, A, Moore, E, Dejong, JD, et al., 2021b. In vitro and in vivo characterization of inosine monophosphate delivered by a nanoparticle in rainbow trout (Oncorhynchus mykiss). N. Am. J. Aquac. https://doi.org/10.1002/naaq.10221.

Kawai, T, Akira, S, 2006. TLR signaling. Cell Death Differ. 13, 816–825. https://doi.org/10.1038/sj.cdd.4401850.

Kaye, M, Druce, J, Tran, T, Kostecki, R, Chibo, D, Morris, J, et al., 2006. SARS-associated coronavirus replication in cell lines. Emerg. Infect. Dis. 12, 128–133.

Kim, S-Y, Noh, Y-W, Kang, TH, Kim, J-E, Kim, S, Um, SH, 2017. Synthetic vaccine nanoparticles target to lymph node triggering enhanced innate and adaptive antitumor immunity. Biomaterials 130, 56–66.

Kouwaki, T, Nishimura, T, Wang, G, Oshiumi, H, 2021. RIG-I-like receptor-mediated recognition of viral genomic RNA of severe acute respiratory syndrome coronavirus-2 and viral escape from the host innate immune responses. Front. Immunol. https://doi.org/10.3389/fimmu.2021.700926.

Lenschow, DJ, Lai, C, Frias-Stahelli, N, Giannakopoulos, NV, Lutz, A, Wolff, T, et al., 2007. IFN-stimulated gene 15 functions as a critical antiviral molecule against influenza, herpes and Sindbis viruses. Proc. Natl Acad. Sci. 104, 1371–1376.

Li, Y, Renner, DM, Comar, CE, Whelan, JN, Reyes, HM, Cardenas-Diaz, FL, Truitt, R, et al., 2021. SARS-CoV-2 induces double-stranded RNA-mediated innate immune responses in respiratory epithelial-derived cells and cardiomyocytes. Proc. Natl Acad. Sci. https://doi.org/10.1073/pnas.2022643118.

McIntosh, K, Dees, JH, Becker, WB, Kapikian, AZ, Chanock, RM, 1967. Recovery in tracheal organ cultures of novel viruses from patients with respiratory disease. Proc. Natl Acad. Sci. 57, 933–940.

Medina, C, Santos-Martinez, MJ, Radomski, A, Corrigan, OI, Radomski, MW, 2007. Nanoparticles: pharmacological and toxicological significance. Br. J. Pharmacol. 150, 552–558.

Menachery, VD, Eisfeld, AJ, Schäfer, A, Josset, L, Sims, AC, Proll, S, et al., 2014. Pathogenic influenza viruses and coronaviruses utilize similar and contrasting approaches to control interferon-stimulated gene responses. ASM. https://doi.org/10.1128/mBio.01174-14.

Milewska, A, Zarebski, M, Nowak, P, Stozek, K, Potempa, J, Pyrc, K, 2014. Human coronavirus NL63 utilizes heparan sulfate proteoglycans for attachment to target cells. J. Virol. https://doi.org/10.1128/JVI.02078-14.

Nikiforuk, AM, Leung, A, Cook, BW, Court, D, Kobasa, D, Theriault, SS, 2016. Rapid one-step construction of a middle east respiratory syndrome (MERS-CoV) infectious clone system by homologous recombination. J. Virol. Methods 236, 178–183.

Owczarek, K, Szczepanski, A, Milewska, A, Baster, Z, Rajfur, Z, Sarna, M, et al., 2018. Early events during human coronavirus OC43 entry to the cell. Sci. Rep. https://doi.org/10.1038/s41598-018-25640-0.

Park, A, Iwasaki, A, 2020. Type I and Type III Interferons – induction, signaling, evasion and application to combat COVID-19. Cell Host Microbe 27, 870–878.

Perng, Y-C, Lenschow, DJ, 2018. ISG15 in antiviral immunity and beyond. Nat. Rev. Microbiol. 16, 423–439.

Persoons, L, Vanderlinden, E, Vangeel, L, Wang, X, Do, NDT, Foo, S-YC, et al., 2021. Broad spectrum anti-coronavirus activity of a series of anti-malaria quinoline analogues. Antiviral Res. https://doi.org/10.1016/j.antiviral.2021.105127.

Pyrc, K, Sims, AC, Dijkman, R, Jebbink, M, Long, C, Deming, D, et al., 2010. Culturing the uncultured: human coronavirus HKU1 infects, replicates, and produces progeny virions in human ciliated airway epithelial cell cultures. J. Virol. 84, 11255–11263.

R Core Team, 2014. R: A language and environment for statistical computing. R Foundation for Statistical Computing, Vienna, Austria. URL. https://www.R-project.org/.

Reed, LJ, Muensch, H, 1938. A simple method of estimating fifty per cent endpoints. Am. J. Epidemiol. 27, 493–497.

RStudio Team, 2015. RStudio: Integrated Development for R. RStudio, Inc., Boston, MA. URL. http://www.rstudio.com/.

Sampaio, NG, Chauveau, L, Hertzog, J, Bridgeman, A, Fowler, G, Moonen, JP, et al., 2021. The RNA sensor MDA5 detects SARS-CoV-2 infection. Sci. Rep. https://doi.org/10.1038/s41598-021-92940-3.

Sa Ribero, M, Jouvenet, N, Dreux, M, Nisole, S, 2020. Interplay between SARS-CoV-2 and the type II interferon response. PLoS Pathog. https://doi.org/10.1371/journal.ppat.1008737.

Schildgen, O, Jebbink, MF, de Vries, M, Pyrc, K, Dijkman, R, Simon, A, et al., 2006. Identification of cell lines permissive for human coronavirus NL63. J. Virol. Methods 138, 207–210.

Scialo, F, Daniele, A, Amato, F, Pastore, L, Matera, MG, Cazzola, M, et al., 2020. ACE2: the major cell entry receptor for SARS-CoV-2. Lung. https://doi.org/10.1007/s00408-020-00408-4.

Sengul, AB, Asmatulu, E, 2020. Toxicity of metal and metal oxide nanoparticles: a review. Environ. Chem. Lett. 18, 1659–1683.

Semple, SL, Au, SKW, Jacob, RA, Mossman, K, DeWitte-Orr, SJ, 2022. Discovery and use of long dsRNA mediated RNA interference (dsRNAi) to stimulate antiviral protection in interferon competent mammalian cells. Front. Immunol. https://doi.org/10.3389/fimmu.2022.859749.

Sodeifian, F, Nikfarjam, M, Kian, N, Mohamed, K, Rezaei, N, 2022. The role of type I interferon in the treatment of COVID-19. J. Med. Virol. https://doi.org/10.1002/jmv.27317.

Sokolova, V, Shi, Z, Huang, S, Du, Y, Kipp, M, Frede, A, et al., 2017. Delivery of the TLR ligand poly(I:C) to liver cells in vitro and in vivo by calcium phosphate nanoparticles leads to pronounced immunostimulation. Acta Biomater. 64, 401–410.

Son, KN, Liang, Z, Lipton, HL, 2015. Double-stranded RNA is detected by immunofluorescence analysis in RNA and DNA virus infections, including those by negative-stranded RNA viruses. J. Virol. 89, 9383–9392.

Speth, MT, Repnik, U, Müller, E, Spanier, J, Kalinke, U, Corthay, A, et al., 2017. Poly(I:C)-encapsulating nanoparticles enhance innate immune responses to the tuberculosis vaccine Bacille Calmette–Guérin (BCG) via synergistic activation of innate immune receptors. Mol. Pharmaceutics 14, 4098–4112.

Totura, AL, Whitmore, A, Agnihothram, S, Schäfer, A, Katze, MG, Heise, MT, et al., 2015. Toll-like receptor 3 signaling via TRIF contributes to a protective innate immune response to severe acute respiratory syndrome coronavirus infection. mBio. https://doi.org/10.1128/mBio.00638-15.

Tyrrell, DA, Almeida, JD, Cunningham, CH, Dowdle, WR, Hofstad, MS, McIntosh, K, et al., 1975. Coronaviridae. Intervirology 5, 76–82.

Tyrrell, DA, Bynoe, ML, 1966. Cultivation of viruses from a high proportion of patients with colds. Lancet 1, 76–77.

Vanderheiden, A, Ralfs, P, Chirkova, T, Upadhyay, AA, Zimmerman, MG, Bedoya, S, et al., 2020. Type I and type III interferons restrict SARS-CoV-2 infection of human airway epithelial cultures. J. Virol. https://doi.org/10.1128/JVI.00985-20.

Van der Hoek, L, 2007. Human coronaviruses: what do they cause? Antivir. Ther. 12, 651–658.

Villeret, B, Dieu, A, Straube, M, Solhonne, B, Miklavc, P, Hamadi, S, et al., 2018. Silver nanoparticles impair retinoic acid-inducible gene I-mediated mitochondrial antiviral immunity by blocking the autophagic flux in lung epithelial cells. ACS Nano 12, 1188–1202.

Wang, C, Zheng, X, Gai, W, Wong, G, Wang, H, Jin, H, et al., 2017. Novel chimeric virus-like particles vaccines displaying MERS-CoV receptor-binding domain induce specific humoral and cellular immune response in mice. Antiviral Res. 140, 55–61.

Wang, N, Zhan, Y, Zhu, L, Hou, Z, Liu, F, Song, P, et al., 2020. Retrospective multicenter cohort study shows early interferon therapy is associated with favorable clinical responses in COVID-19 patients. Cell Host Microbe. https://doi.org/10.1016/j.chom.2020.07.005.

Warnes, SL, Little, ZR, Keevil, CW, 2015. Human coronavirus 229E remains infectious on common touch surface materials. mBio. https://doi.org/10.1128/mBio.01697-15.

Weber, F, Wagner, V, Rasmussen, SB, Hartmann, R, Paludan, SR, 2006. Double-stranded RNA is produced by positive-strand RNA viruses and DNA viruses but not in detectable amounts by negative-sense RNA viruses. J. Virol. 80, 5059–5064.

Yamada, T, Sato, S, Sotoyama, Y, Orba, Y, Sawa, H, Yamouchi, H, et al., 2021. RIG-I triggers a signaling-abortive anti-SARS-CoV-2 defense in human lung cells. Nat. Immunol. https://doi.org/10.1038/s41590-021-00942-0.

Yang, E, Li, MMH, 2020. All about the RNA: interferon-stimulated genes that interfere with viral RNA processes. Front. Immunol. https://doi.org/10.3389/fimmu.2020.605024.

Yeager, CL, Ashmun, RA, Williams, RK, Cardellichio, CB, Shapiro, LH, Look, AT, et al., 1992. Human aminopeptidase N is a receptor for human coronavirus 229E. Nature 357, 420–422.

Zhao, J, Wohlford-Lenane, C, Zhao, J, Fleming, E, Lane, TE, McCray, PB, et al., 2012. Intranasal treatment with poly(I·C) protects aged mice from lethal respiratory virus infections. J. Virol. https://doi.org/10.1128/JVI.01410-12.